Journal of Alloys and Compounds 509S (2011) S572–S575

Contents lists available at ScienceDirect

Journal of Alloys and Compounds

journal homepage: www.elsevier.com/locate/jallcom

Structure modification of Mg–Nb films under hydrogen sorption cycles

P. Mengucci[a,*], G. Barucca[a], G. Majni[a], N. Bazzanella[b], R. Checchetto[b], A. Miotello[b]

[a] Dipartimento di Fisica e Ingegneria dei Materiali e del Territorio, Università Politecnica delle Marche, Via Brecce Bianche, I-60131 Ancona, Italy
[b] Dipartimento di Fisica, Università di Trento, Via Sommarive, I-38123 Povo (TN), Italy

ARTICLE INFO

Article history:
Received 28 July 2010
Received in revised form 9 November 2010
Accepted 10 November 2010
Available online 18 November 2010

Keywords:
Hydrogen storage
Magnesium hydride
Sorption kinetics
Structure modification
Electron microscopy
X ray diffraction

ABSTRACT

In the present work we focus our attention on the structural modifications induced by repeated absorption/desorption cycles on Mg–Nb layers. Samples consisting of a 30 μm thick pure Mg or Mg–5 at.% Nb doped films, coated with a 20 nm thick Pd layer were submitted to repeated H_2 sorption cycles in a volumetric apparatus.

Isothermal desorption analysis at 350 °C was performed to evaluate the amount of absorbed hydrogen. X-ray diffraction (XRD), energy dispersive spectroscopy (EDS) and electron microscopy techniques (SEM and TEM) were used for the structural characterisation of the samples. Analyses show a deep modification of the material upon cycling. The presence of Nb enhances the structural modifications and induces an initial lattice contraction of the Mg matrix that tends to decrease on cycling via the formation of Nb nanoparticles (with average size of ~10 nm). SEM and TEM observations performed in cross section evidenced the formation of a porous structure.

1. Introduction

It is well known from literature that small additions of transition metals (TM) or their oxides (TMO) to a Mg matrix are able to improve the hydrogen sorption kinetics [1]. In our previous works, we reported on the different catalytic effects of various TM additions to a thin film of pure Mg [2–4]. In particular, we found that among the different TM tested, Nb results to be one of the most efficient elements in speeding up the hydrogen kinetics. In recent papers, we proposed a possible mechanism responsible of the catalytic effect of Nb clusters dispersed in a Mg matrix [5], and we also investigated the role of vacancies and vacancy clusters formation on the H_2 kinetics [6]. However, although the catalytic effects of different TMs are clearly known, the microscopic mechanisms leading to the improved sorption kinetics are not fully understood.

In this work, we report on the structure modifications induced by repeated absorption/desorption cycles on pure Mg and 5 at.% Nb-doped layers, aiming to contribute to clarify the microscopic processes responsible of the catalytic effects. Samples obtained by sputtering and submitted to repeated H_2 sorption cycles have been analysed by X ray diffraction (XRD), energy dispersive spectroscopy (EDS), scanning electron microscopy (SEM) and transmission electron microscopy (TEM). The study is based on the comparison between the pure Mg samples and the Nb-doped ones.

2. Experimental

Pure (Mg–Nb0%) and Nb-doped (Mg–Nb5%) Mg films about 30 μm thick were deposited by r.f. magnetron sputtering on graphite in Ar atmosphere. The background pressure in the chamber was about 10^{-5} Pa and the deposition process was carried out at 0.5 Pa Ar pressure and 150 W r.f. power without substrate heating. The target size was 10 cm in diameter while the target to substrate distance was 4 cm. These conditions resulted in a growth rate of about 10 μm/h [7]. Both pure and Nb-doped samples were coated with a 20 nm thick Pd capping layer able to protect samples from surface oxidation and to catalyse the H_2 dissociation kinetics during the hydriding process [8].

After deposition, the samples were peeled off from the graphite substrate. The self supporting samples were thus introduced in a volumetric apparatus for H_2 cycling and for studying the isothermal sorption kinetics at 350 °C [2,4,7].

For the subsequent structural characterisation samples were removed from the volumetric apparatus and exposed to air. Samples submitted to 1, 2, 4, and 8 absorption/desorption cycles, as well as the as-deposited sample as a reference, were characterised by X ray diffraction (XRD), scanning electron microscopy (SEM), transmission electron microscopy (TEM) and energy dispersive spectroscopy (EDS).

XRD analyses were carried out by a Bruker D8 Advance diffractometer in Bragg–Brentano geometry at 40 kV and 40 mA using the Cu-Kα radiation.

Conventional SEM observations were performed by a Philips XL20 electron microscope at 30 kV equipped with an Edax Quanta microanalysis (EDS).

The high resolution observations were carried out by a field emission Zeiss Supra 40 scanning electron microscope.

A Philips CM200 transmission electron microscope at 200 kV equipped with an Edax Phoenix microanalysis (EDS) was used for the TEM observations.

Samples for in plan and cross sectional TEM observations were prepared by conventional thinning procedures. The final thinning was performed by a Gatan precision ion polishing system at 4.5 kV, 0.2 mA and 4° of incidence. Selected area

* Corresponding author.
E-mail address: p.mengucci@univpm.it (P. Mengucci).

0925-8388/$ – see front matter © 2010 Elsevier B.V. All rights reserved.
doi:10.1016/j.jallcom.2010.11.062

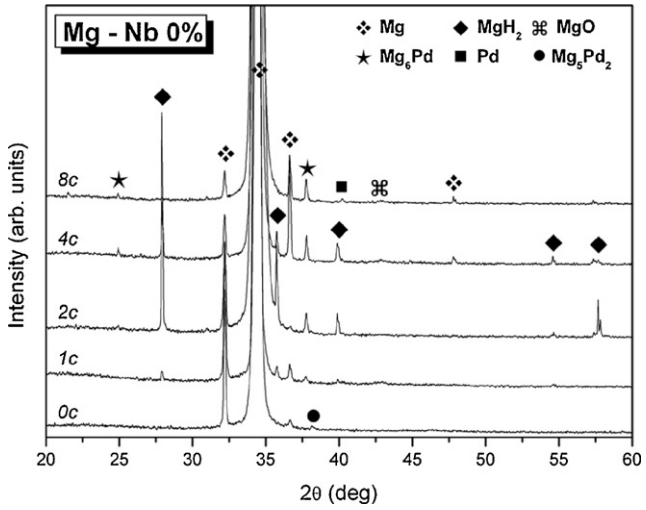

Fig. 1. XRD spectra of the pure Mg sample (Mg–Nb0%) submitted to 1, 2, 4, and 8 H_2 sorption cycles. The 0c curve represents the as-deposited sample.

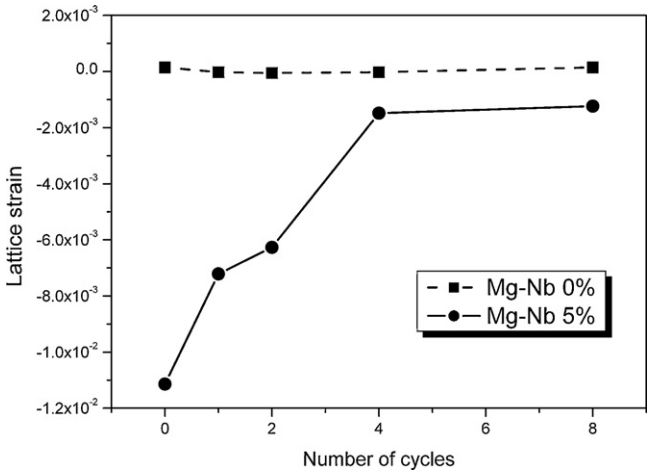

Fig. 3. Lattice strain of the Mg (0 0 2) plane as a function of the sorption cycles. Pure Mg sample (squares), Nb-doped sample (dots).

and convergent beam electron diffraction techniques were used to investigate the local samples crystallographic structure.

Sample composition and its impurity content were obtained by EDS.

3. Results and discussion

The analysis by volumetric technique allows evaluating the amount of hydrogen desorbed from the sample as a function of time. The results obtained clearly show the catalytic effect of Nb. In particular, it is evident from the experimental curves (not shown here) that the Nb-doped sample (Mg–Nb5%) exhibits kinetics ten times faster than pure Mg (Mg–Nb0%). Such results have been already reported and discussed elsewhere [2,4–6,9].

Fig. 1 shows the XRD spectra of the Mg pure sample at different numbers of absorption/desorption cycles up to a maximum of 8. The spectrum named 0c corresponds to the as-deposited sample.

In general, the XRD spectrum of both pure Mg and Nb-doped samples in the as deposited condition as well as after cycling, always shows a most intense peak around $2\theta = 34.4^\circ$ due to the Mg (0 0 2) reflection. The peak intensity suggests a preferential film growth with the *c*-axis of the hexagonal Mg lattice perpendicular to the substrate (axial texture) and a consequent columnar grain structure. The intensity of the Mg (0 0 2) peak tends to decrease upon cycling.

In addition to the Mg reflections, the XRD spectrum of the Mg pure sample in the as-deposited condition (Fig. 1-spectrum 0c) only shows a weak peak at $2\theta = 37.69^\circ$ attributable to the hexagonal Mg_5Pd_2 compound (ICDD card no. 22-713) due to the reaction of the Pd surface layer with the underlying Mg film. Reflections of metallic Pd and magnesium oxides are not visible in the as-deposited sample.

After 1 cycle (Fig. 1-spectrum 1c) the fcc Mg_6Pd compound (ICDD card no. 25-1084) replaces Mg_5Pd_2 while residual peaks of the tetragonal MgH_2 phase (ICDD card no. 12-697) are present. By increasing the number of repeated cycles increases the total amount and the crystalline state of the Mg_6Pd compound.

A weak peak of the metallic Pd (ICDD card no. 6-1043) appears only after 8 cycles (Fig. 1-spectrum 8c) while the presence of MgO (ICDD card no. 45-946) remains always limited.

Different amounts of residual MgH_2 are present in the investigated sample with a clear prevalence for the sample submitted to 2 cycles (Fig. 1-spectrum 2c).

Although few variations in the peak heights are visible, it is remarkable that the general appearance of the different XRD spectra for the pure Mg sample remains almost similar (Fig. 1).

In Fig. 2 the XRD spectra of the Nb doped sample (Mg–Nb5%) after 0, 1, 2, 4 and 8 H_2 sorption cycles are reported. In this case, the as-deposited sample (Fig. 2-spectrum 0c) presents few weak peaks attributable to Mg_5Pd_2 and a reflection around $2\theta = 40.12^\circ$ due to Pd (1 1 1). This latter peak tends to disappear on cycling.

After 1 sorption cycle (Fig. 2-spectrum 1c) sample presents a completely different structure with respect to the as-deposited one (Fig. 2-spectrum 0c). The Mg (0 0 2) peak is now narrower and shifted to smaller angles while a broad diffraction peak around $2\theta = 37^\circ$ is clearly visible. The deconvolution of this broad peak allows distinguishing three main contributions due to Mg (1 0 1), $NbH_{0.89}$ (2 0 0) (ICDD card no. 7-263) and Mg_6Pd. The presence of

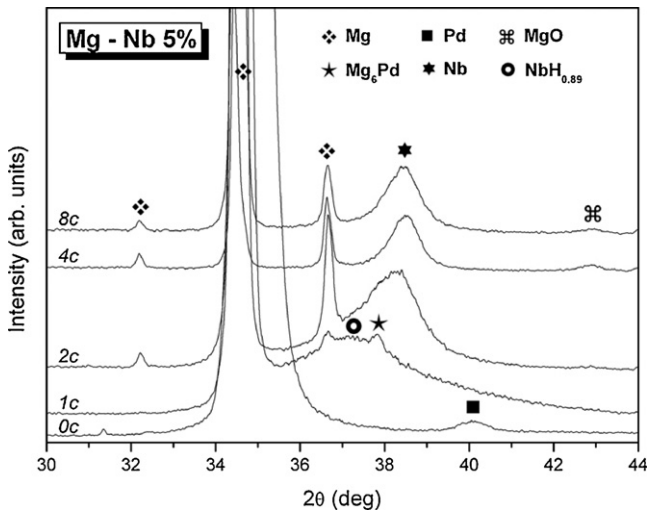

Fig. 2. XRD spectra of the Nb-doped sample (Mg–Nb5%) submitted to 1, 2, 4, and 8 H_2 sorption cycles. The 0c curve represents the as-deposited sample.

Table 1
Average size of the Nb particles formed in the Mg–Nb5% sample after repeated H_2 sorption cycles, as calculated from the XRD spectra.

Number of cycles	Nb particle size (nm)
1	10 ± 1 ($NbH_{0.89}$)
2	10.4 ± 0.8
4	10.8 ± 0.2
8	9.2 ± 0.2

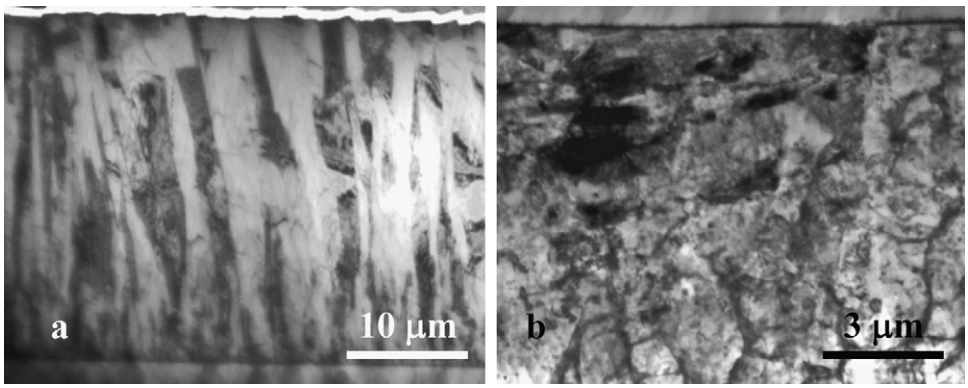

Fig. 4. TEM cross section image of the pure Mg sample: (a) as-deposited (0c) and (b) after 8 sorption cycles (8c).

metallic Nb is not evident from the XRD spectrum (Fig. 2-spectrum 1c).

After 2 repeated sorption cycles (Fig. 2-spectrum 2c) the contribution of the niobium hydride is strongly reduced while a broad peak attributable to Nb (1 1 0) (ICDD card no. 35-789) is now visible.

Increasing the number of cycles leads to the disappearance of the niobium hydride and to a better definition of the Nb peak (Fig. 2-spectra 4c and 8c).

The Mg_6Pd compound is always present and the amount of MgO is always low.

The average dimension of the Nb particles as calculated by applying the Scherrer formula to the deconvoluted $NbH_{0.89}$ (2 0 0) peak (Fig. 2-spectrum 1c) and to the Nb (1 1 0) reflection (Fig. 2-spectra from 2c to 8c) is reported in Table 1. It is worth noting that the average size of the Nb particles does not change markedly upon cycling suggesting a substantial increase of their total number density because of clustering of the still dispersed Nb atoms.

Since the Mg (0 0 2) reflection is always very intense it was used for the estimation of the lattice strain for all the analysed samples. The exact angular position of the Mg (0 0 2) reflection was obtained by a Lorentzian interpolation of the peak and the corresponding interplanar distance (d) was calculated by applying the Bragg law. The lattice strain of the Mg (0 0 2) planes expressed in terms of changes in the interplanar distance was determined by the formula:

$$\varepsilon = \frac{d - d_0}{d_0}$$

where d_0 is the stress-free lattice spacing of the Mg (0 0 2) planes. For the strain estimation we have assumed $d_0 = 0.605$ nm that corresponds to the stress-free value of the Mg (0 0 2) interplanar distance reported in the ICDD card no. 35-381. In this condition, the relative error associated to the lattice strain ε is about 0.15%.

The results are shown in Fig. 3 where symbols refer to pure Mg (solid squares) and Nb-doped samples (solid dots), respectively. From the figure it is clearly evident that the lattice strain of the pure Mg sample (solid squares) remains stable during cycling and almost negligible. On the contrary, the Nb-doped sample (solid dots) shows a relatively high Nb induced lattice contraction in the as-deposited condition (0c) that rapidly drops to small values upon cycling (Fig. 3). This lattice strain relaxation can be ascribed to the combined action of hydrogen cycling and Nb nanoparticle formation. The contribution of thermal cycling is here considered as implicit in the hydrogen cycling one.

While the strain reduction by hydrogen cycling was already observed [10], the contribution of the Nb nanoparticle formation to the lattice strain relaxation can be easily understood. Soon after deposition, Nb is dispersed inside the Mg lattice in solid solution or forms small clusters of few atoms [3], not detectable by XRD analysis, responsible of the Mg lattice contraction. On cycling, the Nb clusters grow in size and density, as already shown by XRD, so contributing to the strain reduction.

Although the catalytic effect of the Nb clusters can be interpreted as in Ref. [5], the presence of a Nb induced lattice contraction in the Mg (0 0 2) planes could give rise to cooperative phenomena, already observed in nano-composite systems as a consequence of the elastic interactions [11–13]. Therefore, the lattice strain present in the Nb-doped samples can influence the H_2 sorption kinetics before the complete lattice strain relaxation.

Cross sectional TEM observation of the samples in the as-deposited condition shows the columnar grain structure and allows measuring the total thickness of the deposited Mg and Pd layers that are in agreement with the nominal values, i.e. about 30 μm and 20 nm, respectively.

Fig. 4(a) shows the structure of the pure Mg sample in the as-deposited condition. The Mg grains grow in columnar form and extend through the entire layer thickness; their lateral dimension ranges from 0.5 to 3 μm.

After 8 repeated sorption cycles, the Mg pure sample appears as in Fig. 4(b). The columnar grain structure is roughly maintained but many large pores distributed throughout the material are now present.

Selected area electron diffraction patterns confirmed the presence of Mg_5Pd_2 and Mg_6Pd at the interface between the surface Pd layer and the underlying Mg.

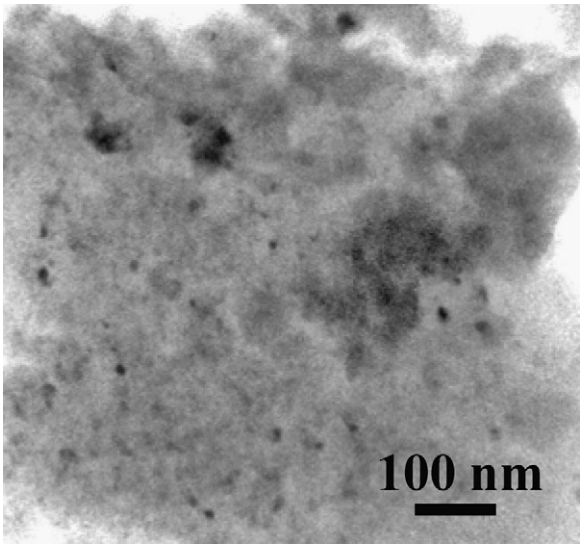

Fig. 5. TEM micrograph of the Mg–Nb5% sample after 8 sorption cycles.

On repeated H_2 sorption cycles, the Nb-doped sample develops a porous structure much more pronounced than that observed in the pure Mg samples. On cycling the porous structure becomes more and more evident both in TEM and SEM images. It is worth to note that the porous structure tends to spread by increasing the sorption cycles and the pores are always preferentially located in the regions with a high Nb particle density. This effect can be explained considering that the interface between the Nb nanoclusters and the MgH_2 acts as a preferential nucleation site for Mg in the hydride to metal phase transition [5]. Due to the local high Nb particle density, hydrogen from the dissociated hydride phase here reaches a concentration larger than the maximum H solubility in the Mg matrix. Consequently a fraction of the H atoms is trapped in extended defects here present (dislocations or vacancy clusters at the Mg–Nb interface) and give rise to the damage effects.

Fig. 5 reports the distribution of the Nb particles for the sample submitted to 8 sorption cycles. The average size of the particles is 10 nm in agreement with the results of the XRD analysis (Table 1).

The presence and the evolution of the porous structure in the pure Mg samples as well as in the Nb-doped ones suggest a correlation between the mechanisms involved in the Mg–MgH_2 transformation and the pores formation.

Further work is in progress to clarify the role of the extended pores on the H_2 sorption kinetics.

4. Conclusions

In this paper we report the results obtained by different analytical techniques on the structure modifications induced by repeated hydrogen sorption cycles on pure Mg and 5 at.% Nb–Mg doped film, coated with a thin Pd layer.

Analyses show that the sorption cycles and the presence of Nb induce remarkable changes on the sample microstructure. The main results can be summarised as follows:

- a Nb induced lattice contraction that tends to decrease upon cycling characterises the Nb-doped samples; the strain relaxation occurs by a combined effect of the thermal and hydrogen cycling that promotes the formation of Nb nanoparticles (about 10 nm in size);
- a widespread porous structure appears in the samples upon cycling; it is much more pronounced in the Nb-doped samples and preferentially located in the regions with a higher density of Nb nanoparticles;
- cooperative phenomena induced by the lattice strain can contribute to accelerate the hydrogen sorption kinetics in the Nb-doped samples.

Further work is in progress to correlate the above results to the hydrogen storage efficiency and to the H_2 sorption kinetics.

References

[1] B. Sakintuna, F. Lamari-Darkrim, M. Hirscher, Int. J. Hydrogen Energy 32 (2007) 1121.
[2] R. Checchetto, N. Bazzanella, A. Miotello, P. Mengucci, J. Alloys Compd. 446–447 (2007) 58.
[3] R. Checchetto, N. Bazzanella, A. Miotello, C. Maurizio, F. D'Acapito, P. Mengucci, G. Barucca, G. Majni, Appl. Phys. Lett. 87 (2005) 061904.
[4] N. Bazzanella, R. Checchetto, A. Miotello, C. Sada, P. Mazzoldi, P. Mengucci, Appl. Phys. Lett. 89 (2006) 014101.
[5] R. Checchetto, N. Bazzanella, A. Miotello, P. Mengucci, J. Phys. Chem. Solids 69 (2008) 2160.
[6] L. Toniutti, R. Checchetto, P. Mengucci, A. Miotello, R.S. Brusa, Phys. Stat. Solidi C 6 (2009) 2310.
[7] R. Checchetto, G. Trettel, A. Miotello, Meas. Sci. Technol. 15 (2004) 127.
[8] R. Checchetto, N. Bazzanella, A. Miotello, R.S. Brusa, A. Zecca, P. Mengucci, J. Appl. Phys. 95 (2004) 1989.
[9] R. Checchetto, N. Bazzanella, A. Miotello, P. Mengucci, J. Alloys Compd. 404–406 (2005) 461.
[10] B. Paik, A. Walton, V. Mann, D. Book, I.P. Jones, I.R. Harris, J. Alloys Compd. 35 (2010) 9012.
[11] K. Higuchi, K. Yamamoto, H. Kajioka, K. Toiyama, M. Honda, S. Orimo, H. Fujii, J. Alloys Compd. 330–332 (2002) 526.
[12] S. Orimo, H. Fujii, K. Ikeda, Acta Mater. 45 (1997) 331.
[13] H. Fujii, S. Orimo, K. Ikeda, J. Alloys Compd. 253–254 (1997) 80.